Journal of Applied Fluid Mechanics, Vol. 11, No. 3, pp. 613-620, 2018.
Available online at www.jafmonline.net, ISSN 1735-3572, EISSN 1735-3645.
DOI: 10.29252/jafm.11.03.28246

Effect of Pitch Angle and Reynolds Number on Aerodynamic Characteristics of a Small Horizontal Axis Wind Rotor

J. Y. Zhu[1,2†] and P. Q. Liu[1]

[1] *Key Laboratory of Fluid Mechanics, Ministry of Education, Beihang University, Beijing, 100083, China*
[2] *Faculty of Aerospace Engineering, Shenyang Aerospace University, Shenyang, Liaoning Province, 100136, China*

†*Corresponding Author Email: michellend@126.com*

(Received July 23, 2017; accepted December 5, 2017)

ABSTRACT

Wind tunnel experiments were conducted on a 2-blade horizontal axis wind rotor to investigate the effect of pitch angle and Reynolds number on aerodynamic characteristics. The experimental study was conducted in the start-up and operating stages and the results for the two stages are discussed, respectively. During start-up, with tip speed ratio less than 1, the power coefficient of the rotor increases with pitch angles, but remains almost constant with Reynolds number. In the operating stage, with tip speed ratio more than 1, the maximum power coefficient occurs at decreasing tip speed ratios as the pitch angle increases. In addition, the maximum power coefficient increases and the corresponding tip speed ratio decreases with Reynolds number. The aerodynamic characteristics of the rotor can be analyzed qualitatively based on reliable and full aerodynamic data of the airfoil, which contributes to selection of the airfoil and determination of the rated velocity.

Keywords: Wind energy; Horizontal axis wind rotor; Reynolds number; Aerodynamic characteristics; Wind tunnel test.

1. INTRODUCTION

Wind energy is one of fastest growing and among the most promising renewable energy sources of the world. In the light of increasing concern about energy shortage and environmental protection in urban areas, onsite utilization of wind energy in the urban environment is an effective solution (Zhu *et al*. 2017, Karthikeyan *et al*. 2015). In contrast to large scale wind turbines that are located in remote areas and driven by abundant wind resources, small wind turbines are more appropriate for urban environment where they are located closed to where power is needed, rather than where the wind is most favorable (Singh *et al*. 2012, Dayan 2006).

Wind in the urban environment characterized by low wind speeds, high levels of turbulence and unsteady direction and speed (Ledo *et al*. 2011, Wang *et al*. 2008). In such environment, the aerodynamic problems of the wind turbines involve dynamic unsteadiness, low operating Reynolds number and the need for high angles of attack (Wright *et al*. 2004). The small wind turbine is usually designed to operate at between 3 and 15 m/s, and the operating Reynolds number based on blade chord and inflow velocity is almost between 10^5 to 5×10^5 (Islam *et al*. 2007). At low Reynolds numbers, laminar separation occurs near the leading edge of the turbine blade and degrades the overall aerodynamic performance of the turbine (Singh *et al*. 2013, Ozgener *et al*. 2007). In addition, the start-up of small horizontal-axis wind turbines purely depends on the torque produced by the wind acting on the rotor. Small horizontal-axis wind turbines are of fixed pitch in consideration of cost and complexity of the mechanism (Pourrajabian *et al*. 2014). A relatively large pitch is usually selected for startup Therefore, low Reynolds number and large pitch are two of vital parameters influencing the aerodynamic performance of small horizontal-axis wind turbines.

In allusion to the aerodynamic problems mentioned above, there have been many studies on the effect of Reynolds number and pitch on the aerodynamic characteristics of the airfoil and the horizontal wind turbine. Based on this characteristic of the airfoil, a low Reynolds number airfoil was designed by Singh *et al.* (2013) for application in small □□□izontal axis wind turbines to achieve better startup and low speed performance. Freudenreich *et al.* (2004) studied the effect of Reynolds number and roughness on thick airfoils (DU97-300mod) for

wind turbine, the results showed that the maximum lift-to-drag ratio was independent of *Re* between 10^6 and 10^7. Sheldahl *et al.* (1981) conducted a series of wind tunnel tests for four symmetrical airfoils at moderate values of *Re* from 10^4 to 10^7, obtaining the aerodynamic force and moment data among the entire range of angles of attack (-180° to +180°). Worasinchai *et al.* (2011) tested four appropriate airfoils at three Reynolds numbers (6.5×10^4, 9×10^4, 1.5×10^5), and obtained the aerodynamic performance of the airfoil in terms of lift, drag and static pressure coefficients, the results showed that both geometry and Reynolds number had significant effects on aerodynamic lift. As for the horizontal axis wind turbine, Sahin *et al.* (2001) designed a 100W small-scale and tested power output in a low-speed wind tunnel without considering effect of Reynolds number and profile parameters. Kishinami *et al.* (2005) investigated the aerodynamic characteristics of the different three type of HAWT blades for values of pitch, namely pitch 1°, 4° and 7°, and observed that the occurrence of maximum power coefficient and the corresponding tip velocity ratio decreased with the increase of the pitch for tip speed ratio between 3 and 10. Driss *et al.* (2013) examined the Reynolds number effect on the aerodynamic characteristics of a horizontal axis wind turbine and found that the Reynolds number had a direct effect on the global characteristics, except the static torque coefficient, and power coefficient increases with Reynolds number at the same specific tip speed ratio, however, the maximum power coefficient was not tested as well as the ones at low tip speed ratio. Mctavish *et al.* (2013) evaluated Reynolds number effect on thrust coefficient and initial wake expansion for small–scale wind turbine, observing that the thrust coefficient increases with Reynolds number.

Available research on the effect of Reynolds number and pitch angle mostly concerns the aerodynamic characteristics of wind turbines with the large tip velocity ratios, and pay little attention to relatively low tip velocity ratios. Thus, further exploration is necessary to know the aerodynamic characteristics of wind turbines at low tip speed ratios. The objective of this study is to measure the power performance in the full operating range of tip velocity ratio of a small horizontal axis wind turbine for free stream velocities and pitch angles to evaluate the effect of Reynolds number and pitch angle. Furthermore, the main causes of the change of aerodynamic characteristics have been analyzed in detail in terms of the element theory combining aerodynamic data of the airfoil.

2. THEORETICAL ANALYSIS

The blade element at radial position r is intercepted parallel to the flow direction, as shown in Fig. 1, which also shows the velocity components. It is assumed that no velocities are induced by the relatively small power generated by the wind turbine. V_∞ is the freestream velocity, ω is the rotational angular velocity, the pitch angle θ is the angle between blade rotation plane and chord line. The incoming flow angle ϕ, defined by $\phi = a\cot(r\omega/V_\infty)$, is the angle of resultant velocity $W_r = \sqrt{V_\infty^2 + (\omega r)^2}$ to the blade rotation plane, which equals the sum of θ and local angle of attack α. The tip speed ratio λ is defined by

$$\lambda = R\omega/V_\infty \tag{1}$$

where R is the wind rotor radius.

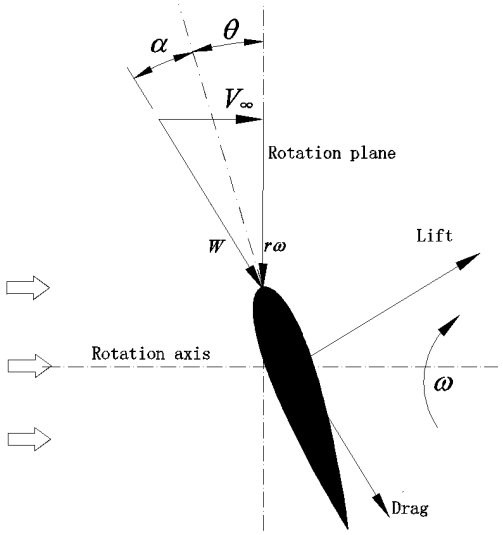

Fig. 1. Blade element, velocity components.

For a wind rotor, the power coefficient Cp is used to evaluate the effectiveness of utilization of wind energy and depends on tip speed ratio λ, pitch angle θ and Reynolds number Re, and is given as follows:

$$Cp(\lambda,\theta,Re) = M\omega/(0.5\rho V_\infty^3 \pi R^2) \tag{2}$$

where M is the aerodynamic torque, ρ is the air density.

$\bar{r}$ is defined the normalized local radius in terms of $\bar{r} = r/R$ to simplify expressions of $\phi = a\cot(r\omega/V_\infty)$ and facilitate the later analysis Thus the incoming flow angle ϕ is also presented by $\phi = a\cot(\lambda\bar{r})$, which indicates ϕ is mainly correlated to tip speed ratio λ, and ϕ decreases as $\bar{r}$ increases. The existence of pitch angele decides the local angle of attack α, directly affect the aerodynamic characteristics of the rotor.

Besides, the variation of resultant velocities and chord lengths with radial position of blade lead to variation of local Reynolds numbers in terms of $Re_r = \rho c_r W_r/\mu$, where ρ is air density, μ is dynamic viscosity coefficient, and c_r is the local chord length.

Low Reynolds numbers are subject to uncertainty even in the steady flow past airfoils. Figs. 2a and 2b show the lift and drag coefficients for NACA0018 for $10^4 < Re < 5 \times 10^6$, respectively, and it is evident that the lift increases and drag decreases with *Re* for small angles of attack. However, the aerodynamic characteristics of any airfoil at high angles of attack are like those of flat plate, so that for NACA0018, the lift for $\alpha > 35°$ and drag for $\alpha > 20°$ do not change with Reynolds number. For smaller angles of attack and low Reynolds number, the Reynolds number will be an important factor determining the aerodynamic characteristics of the wind turbines.

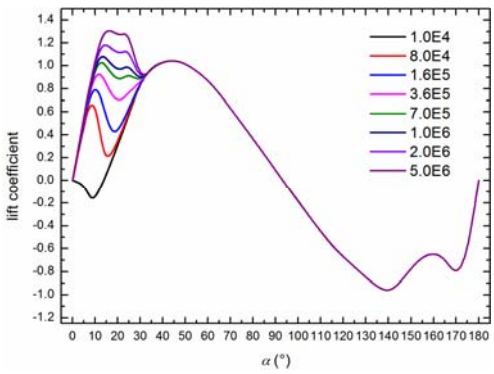

(a) Lift coefficient

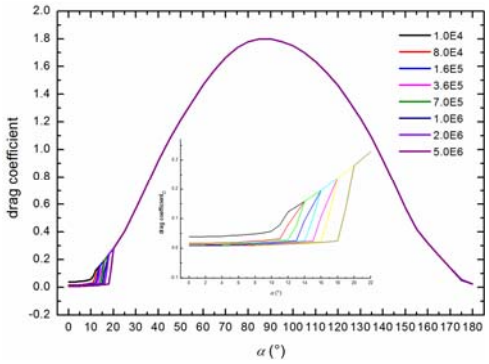

(b) Drag coefficient

Fig. 2. Lift and drag coefficient of NACA 001811.

3. WIND TUNNEL EXPERIMENTAL SET-UP

3.1 Experimental Model and Test Apparatus

The two-bladed horizontal axis wind turbine model shown in Fig. 3 was used to investigate the effect of pitch angle and Reynolds number on aerodynamic characteristics. The cross-sectional profile of the rotor blade is selected of NACA0018 with equal chord and no twist. The wind turbine has a blade length *L* of 270 mm and a chord length *c* of 55 mm. The wind turbine radius *R* is 300 mm, which results in a tunnel blockage of 23.5%.

The experiment was conducted in a low speed wind tunnel at Shenyang Aerospace University. The rectangular cross section of the 3.0 m long wind tunnel test section is 1.0 m high by 1.2 m wide. Using a closed-loop adjusting system to control wind velocity, a steady wind velocity between 3 m/s and 55 m/s was attainable in the test section with flow turbulence intensity less than 0.14%. Figure 3 also identifies the prime measurement equipment utilized in the experiment. The blades were attached to a hub and the pitch angle was adjustable. A torque and rotation speed sensor was used to measure the instantaneous torque and the rotational speed of the wind rotor, the measuring ranges of torque and rotation speed being 0 - 3 Nm and 0 - 6000 rev/min to precision of 0.30% (F.S) and ±0.1%, respectively, under operating conditions. The load was applied with a magnetic powder brake (MPB), which also changed the rotation speed of the wind rotor. The total frictional torque was less than 0.03 Nm. The rotor, sensor and PMB were connected axially, which were fixed to the support. The rotor rotation axis aligned with the center line of the tunnel test section.

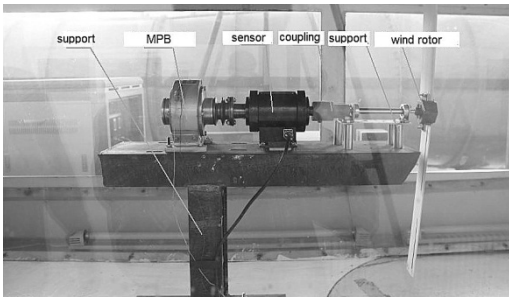

Fig. 3. Wind rotor and measurement equipment.

3.2 Experimental Conditions

The study mainly focuses on determining the effect of Reynolds number and pitch angle on aerodynamic characteristics of the rotor in start-up stage ($\lambda < 1$) and operating stage ($\lambda > 1$), respectively. The power coefficient of the rotor is relatively low in start-up stage, however, the rotor runs most of time in start-up stage and the amount of long-pending power is not ignorable.

The rotation speed, torque and power were collected in conditions of different wind velocities of 10 - 20 m/s and pitch angles of 6°, 8° and 10°. The selection of relatively large wind velocity enables the small-scale rotor model to operating at Reynolds number of 10^5, which approaches the actually operating Reynolds number. The selection of relative small pitch angle also approaches the practical situation, and contributes to attaining higher rotational speed, which is in favor of collecting more data. Owing to the large number of test conditions, the wind velocity and the rotor rotation speed needed to be varied. The data acquisition was carried out when wind velocity and rotor operation were stable. The data sampling frequency is 10 HZ. To offset the fault of low sampling frequency, the sampling time prolongs and the time-averaged rotation speed, torque and power are obtained. The power coefficients versus tip speed ratios under different test conditions are computed using Eqs. (1) - (2).

4. EXPERIMENTAL RESULTS AND DISCUSSION

4.1 Pitch Angle Effect

Three pitch angles of 6°, 8°and 10° are selected to investigate the pitch angle effect on the rotor aerodynamic characteristics in terms of Cp. The pitch angle effect during start-up stage and operating stage is discussed separately.

During start-up stage ($\lambda < 1$), Fig. 4 presents the relationships between Cp and λ under two different wind velocities of 18 m/s and 19 m/s , respectively. In this stage, the curve of Cp almost increases linearly with the crease of λ, but the Cp is relatively small, less than 1%. The curve of Cp also increases with increasing pitch angle, while the increment of Cp decreases.

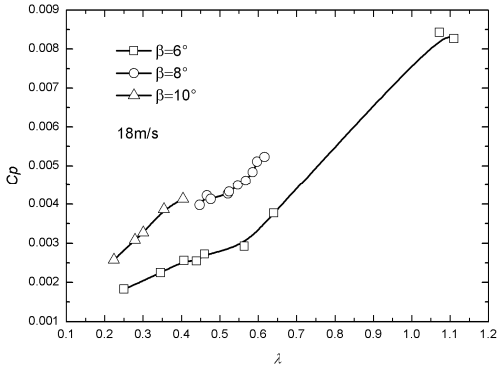

(a) V_∞=18 m/s

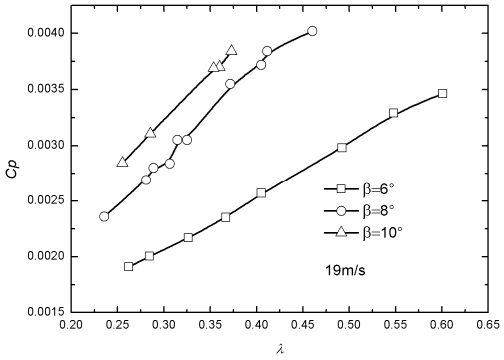

(b) V_∞=19 m/s

Fig. 4. Relationship between Cp and λ for three pitch angles with $\lambda < 1$.

During operating stage ($\lambda > 1$), Fig. 5 presents the relationship between Cp and λ for four wind velocities of 10, 11, 12 and 13 m/s, respectively. The curve of Cp firstly increases and then decreases with λ for all operating conditions, and the maximum power coefficient $Cp_{\max}$ always exceeds 0.1. For any given wind velocity, $Cp_{\max}$ and the corresponding λ decrease with pitch angle and, the effect of the pitch angle on Cp decreases with increase in pitch angle. The results are consistent with observations of Kishinami *et al.* (2005).

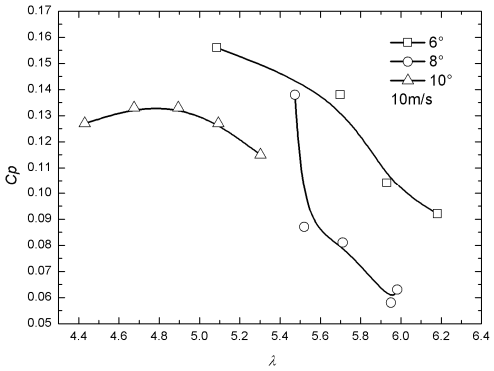

(a) V_∞=10 m/s

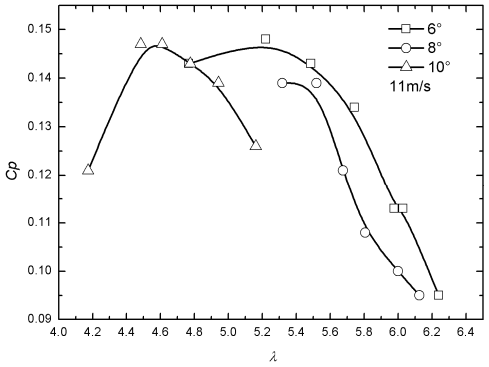

(b) V_∞=11 m/s

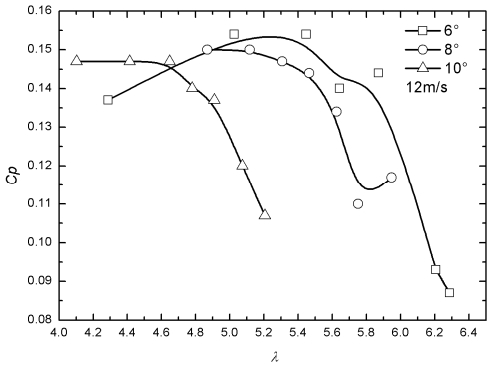

(c) V_∞=12 m/s

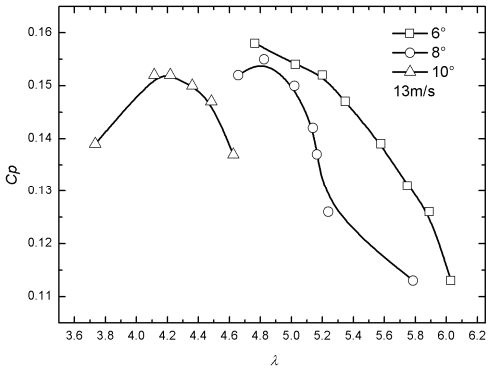

(d) V_∞=13 m/s

Fig. 5. Relationship between Cp and λ for three pitch angles for $\lambda > 1$.

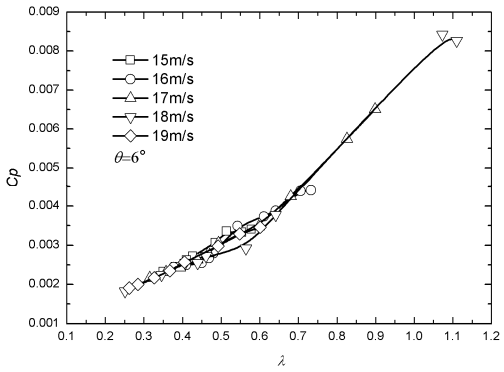

(a) θ =6°

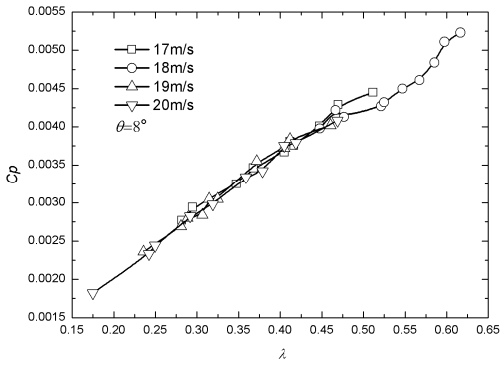

(b) θ =8°

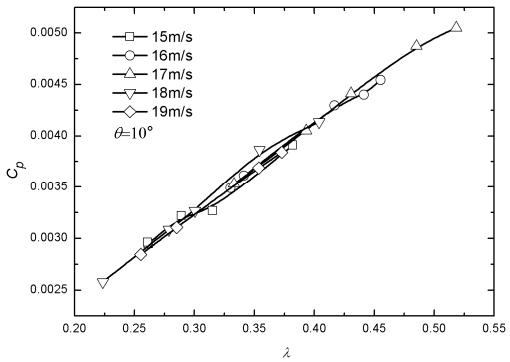

(c) θ =10°

Fig. 6. Relationship between Cp and λ for different wind velocities during $\lambda < 1$.

4.2 Reynolds Number Effect

As stated above, the Reynolds number is a function of freestream wind velocity, and the nominal Reynolds number Re^* is defined based on freestream wind velocity, and its effect on the Cp of the rotor was studied by changing wind velocity. The selected wind velocity varied from 10 to 20 m/s.

Figure 6 presents the relationship between Cp and λ during the start-up stage ($\lambda < 1$), for three values of pitch angle namely 6°, 8° and 10°, respectively. The curves for Cp at different wind velocities almost coincide, indicating that the aerodynamic characteristics of the rotor are not affected by Reynolds number.

Figure 7 presents the relationships between Cp and λ during the operating stage ($\lambda > 1$), for three values of pitch angle namely 6°, 8° and 10°, respectively. It can be seen that as $Cp_{\max}$ increases, the corresponding λ decreases with wind velocity. Also the effect of Reynolds number on Cp increases with pitch angle, and it can be seen that the effect of Reynolds number for a pitch angle of 10° is significantly more than that for a pitch angle of 6°.

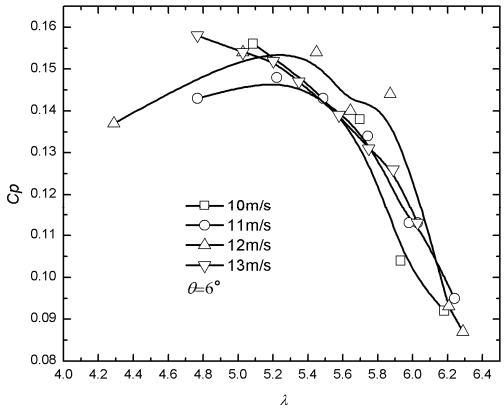

(a) θ =6°

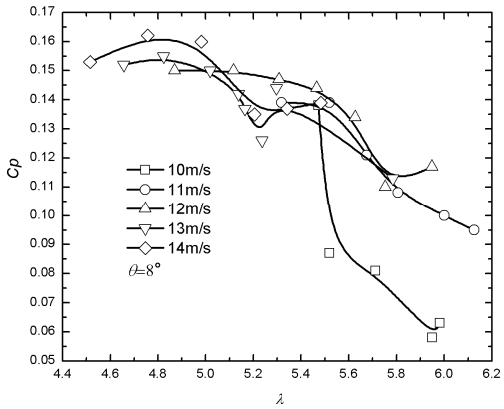

(b) θ =8°

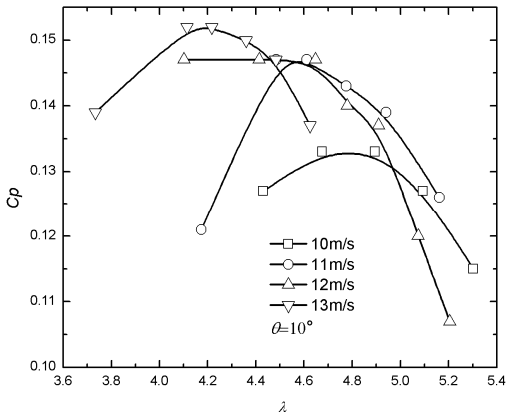

(c) θ =10°

Fig. 7. Relationship between Cp and λ for different wind velocities for $\lambda > 1$.

5. ANALYSIS OF MECHANISM

In order to facilitate analysis, the variation of the local angle of attack α and local Reynolds number Re_r and λ along the radical direction of the blade are shown in Figs. 8 and 9 for the case of θ = 0°, V_∞ = 20 m/s.

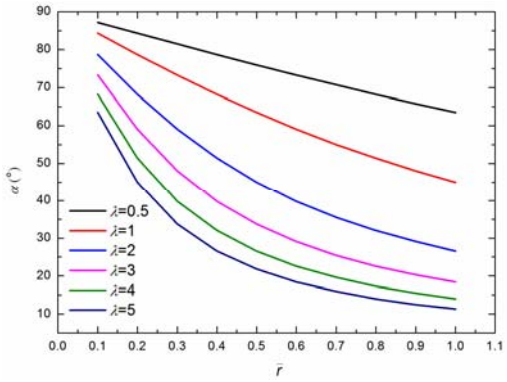

Fig. 8. Local angle of attack along the radial direction.

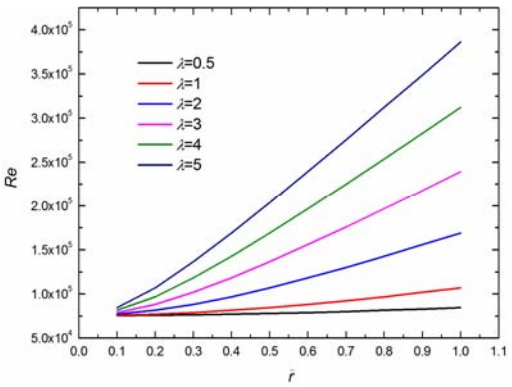

Fig. 9. Local Reynolds number along the radial direction.

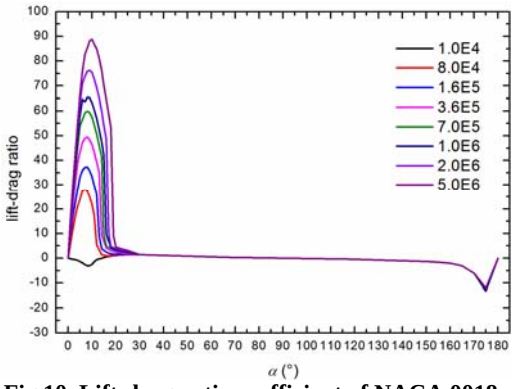

Fig.10. Lift-drag-ratio coefficient of NACA 0018.

5.1 Pitch Angle Effect

Figure 8 shows that the local angle of attack α decreases radically along the blade. The value of α at the blade root remains essentially a constant at 90° as the angular velocity at the blade root is 0 rad/sec; further away, α decreases with tip speed ratio. The change in α with position is increasingly marked with increase in λ.

The minimum α at blade tip during $\lambda<1$ is 45°and the ranges of values of α along the blade corresponding to θ =6°, 8° and 10° are 39° to 84°, 37° to 82° and 35° to 80°, respectively. That is, a blade with relatively high θ has a narrower range of α. Figure 10 presents the lift-drag-ratio curve of NACA 0018, the lift-to-drag ratio for α above 30° decreases with α, so that the overall lift-drag-ratio of the blade with higher θ is higher, leading to higher power coefficient of the rotor.

For $\lambda>1$, especially $4<\lambda<6$, α at blade tip region approaches 5° - 15° namely the optimal range of α, at which the lift-drag-ratio is relatively large and the peak lift-drag-ratio exists in, resulting in maximum power coefficient. As values of θ increase, the optimal range of α is transferred onto inner region of the blade, the corresponding arm of force decreases, resulting in the decrease of power coefficient. In order to obtain maximum power coefficient for large θ, the rotational velocity needs to be lower, so that the optimal range of α is regained at blade tip region. Therefore the maximum power coefficient of rotor is obtained at lower λ.

5.2 Reynolds Number Effect

It is evident from Fig. 10 that the lift-drag-ratio of NACA 0018 and the angle of attack corresponding to peak lift-drag-ratio increase, the range of tip speed ratio of relatively large lift-drag-ratio is broaden with Reynolds number for $0°\leq\alpha\leq30°$, while the lift-drag-ratio does not change with Reynolds number for α >30°.

For $\lambda<1$, the local angles of attack at different radical locations of blade exceed 30°, at which the lift, drag and lift-drag-ratio almost do not change with Reynolds number. Therefore, it is derived from Eq. (2) that the power coefficient of the rotor is independent of Reynolds number.

For $\lambda>1$, especially $4<\lambda<6$, the local angle of attack along blade radical direction dramatically decreases, from 90° at blade root to about 15° at blade tip. The cause of relationship between power coefficient and tip speed ratio is first analyzed. As λ increases, the local angles of attack at different radical locations of blade decrease, until α at blade tip reaches the optimal α, namely the α corresponding to the peak lift-drag-ratio, the total aerodynamic force of the blade increase and the arm of force shifts radically outwardly, therefore the power coefficient increases. As λ goes on increasing, the radical location with the optimal α shifts radically inwardly, α at the blade tip region is gradually less than the optimal α, but the blade tip region still generates relative aerodynamic force, the total aerodynamic force increases and the arm of

force maybe not decrease, thus the power coefficient continues increasing, until reaches the maximum power coefficient $Cp_{\max}$. When λ exceeds that corresponding to $Cp_{\max}$, the radical location with the optimal α continues shifting radically inwardly and the region with α much less than the optimal α enlarges along the radical direction, the total aerodynamic force begins to slip and the arm of force gradually shortens, resulting in the decrease of power coefficient.

The next, the cause of effect of Reynolds number on power coefficient is analyzed. Owing to the optimal range of α being wider, α at the right boundary of the range being larger and the lift-drag-ratio being higher for higher Reynolds number, the larger region of the blade is subjected to higher aerodynamic force under lower λ. That is, the higher power coefficient of the rotor can be obtained at lower λ for higher Reynolds number.

The range of angle of attack along the radical direction of the blade corresponding to different λ is wider for θ=10°, which implies a more significant effect of Reynolds number on the aerodynamic characteristics of the rotor.

6. CONCLUSION

The aerodynamic characteristics of 2-blade horizontal axis wind rotor was investigated in a low speed wind tunnel. The effect of pitch angle and Reynolds number on aerodynamic characteristics has been interpreted, based on the variation of local Reynolds number and local angle of attack along the radical position of the blade and aerodynamic data of NACA 0018 at full angles of attack.

(1) The local angle of attack changes with pitch angle thereby directly affecting aerodynamic characteristics of the rotor. For $\lambda<1$, as pitch angle increases , Cp as well as the corresponding torque coefficient CM increase which indicates that large pitch angle contributes to start-up of the rotor. For $\lambda>1$, the $Cp_{\max}$ is obtained at lower λ as pitch angle increases.

(2) The effect of Reynolds number on aerodynamic characteristics of the rotor is indirectly achieved through Reynolds number affecting aerodynamic lift and drag of the airfoil. For $\lambda<1$, Cp is almost constant in Reynolds number. For $\lambda>1$, $Cp_{\max}$ increases and the corresponding λ decreases as Reynolds number increases.

(3) The aerodynamic characteristics of the rotor can be analyzed qualitatively based on the aerodynamic characteristics of the selected airfoil used for the rotor. The maximum lift-drag-ratio and the corresponding angle of attack of the airfoil determines $Cp_{\max}$ and λ of the rotor, respectively. The higher maximum lift-drag-ratio contributes to higher $Cp_{\max}$, while the larger corresponding angle of attack leads to lower corresponding λ.The range of the optimal α determines the range of relative high Cp in proportion. Besides, the selection of the rated wind velocity for the rotor needs to be cautious. Higher rated wind velocity implies higher Reynolds number so as to obtain higher $Cp_{\max}$ at lower λ.

REFERENCES

Dayan, E. (2006). Wind energy in buildings. *Refocus* 7, 33–38.

Driss, Z., S. Karray, A. Damak and M. Salah Abid (2013). Experimental Investigation of the Reynolds Number's Effect on the Aerodynamic Characteristics of a Horizontal Axis Wind Turbine of the Göttingen 188 Airfoil Type. *American Journal of Mechanical Engineering* 1, 143–148.

Freudenreich, K., K. Kaiser, A. P. Schaffarczyk, H. Winkler and B. Stahl (2004). Reynolds number and roughness effects on thick airfoils for wind turbines. *Wind Engineering* 28, 529–546.

Islam, M., M. R. Amin, S. K. Ting and F. Amir (2007). Aerodynamic Factors Affecting Performance of Straight-Bladed Vertical Axis Wind Turbines. *ASME 2007 International Mechanical Engineering Congress and Exposition* 47, 13-23.

Karthikeyan, N., K. Kalidasa Murugavel, S. Arun Kumar and S. Rajakumar (2015). Review of aerodynamic developments on small horizontal axis wind turbine blade. *Renewable and Sustainable Energy Reviews* 42, 801–822.

Kishinami, K., H. Taniguchi, J. Suzuki, H. Ibano, T. Kazunou and M. Turuhami (2005). Theoretical and experimental study on the aerodynamic characteristics of a horizontal axis wind turbine. *Energy* 30, 2089–2100.

Ledo, L., P. B. Kosasih and P. Cooper (2011). Roof mounting site analysis for micro-wind turbines. *Renewable Energy* 36, 1379–1391.

McTavish, S., D. Feszty and F. Nitzsche (2013). Evaluating Reynolds number effects in small-scale wind turbine experiments. *Journal of Wind Engineering and Industrial Aerodynamics* 120, 81–90.

Ozgener, O. and L. Ozgener (2007). Exergy and reliability analysis of wind turbine systems: a case study. *Renewable and Sustainable Energy Reviews* 11, 1811-1126.

Pourrajabian, A., M. Mirzaei, R. Ebrahimi and D. Wood (2014). Effect of air density on the performance of a small wind turbine blade: A case study in Iran. *Journal of Wind Engineering and Industrial Aerodynamics* 126, 1–10.

Sahin, A. Z., A. Z. Al-Garni and A. Al-Farayedhi (2001). Analysis of a small horizontal axis wind turbine performance. *International Journal of Energy Research* 25, 501–506.

Sheldahl, R. E and P. C. Klimas (1981). Aerodynamic Characteristics of Seven Symmetrical Airfoil Sections Through 180-Degree Angle of Attack for Use in Aerodynamic Analysis of Vertical Axis Wind Turbines. Sandia National Laboratories. Report SAND80-2114.

Singh, R. K. and M. R. Ahmed (2013). Blade design and performance testing of a small wind turbine rotor for low wind speed applications. *Renewable Energy* 50, 812–819.

Singh, R. K., M. R. Ahmed, M. A. Zullah and Y. H. Lee (2012). Design of a low Reynolds number airfoil for small horizontal axis wind turbines. *Renewable Energy* 42, 66–76.

Wang, F., L. Bai, J. Fletcher, J. Whiteford and D. Cullen (2008). The methodology for aerodynamic study on a small domestic wind turbine with scoop. *Journal of Wind Engineering and Industrial Aerodynamics* 96, 1–24.

Worasinchai, S., G. Ingram and R. Dominy (2011). A low-Reynolds-number, high-angle-of-attack investigation of wind turbine airfoils. *Proceedings of the Institution of Mechanical Engineers, Part A: Journal of Power and Energy* 225, 748–763.

Wright, A. K. and D. H. Wood (2004). The starting and low wind speed behaviour of a small horizontal axis wind turbine. *Journal of Wind Engineering and Industrial Aerodynamics* 92, 1265–1279.

Zhu, J. Y., J. M. Wang and P. Q. Liu (2017). Theoretical Analysis and Experimental Investigation of Static Torque Characteristic for H-Darrieus Wind Turbine. J*ournal of Mechanical Engineering* 53(2) , 150–156.